Editors' Suggestion

Disentanglement-induced multistability

Eyal Buks*

Andrew and Erna Viterbi Department of Electrical Engineering, Technion, Haifa 32000, Israel

(Received 4 April 2024; revised 27 May 2024; accepted 28 June 2024; published 15 July 2024)

Multistability cannot be derived from any theoretical model that is based on a monostable master equation. On the other hand, multistability is experimentally observed in a variety of quantum systems. A master equation having a nonlinear term that gives rise to disentanglement has been recently proposed. The dynamics governed by this master equation is explored for a quantum system made of coupled spins. It is found that the added nonlinear term can give rise to multistability. The spins' response to an externally applied magnetic field is evaluated, and both a phase transition and a dynamical instability are found. These findings, which originate from disentanglement-induced multistability, indirectly support the hypothesis that spontaneous disentanglement occurs in quantum systems.

DOI: 10.1103/PhysRevA.110.012439

I. INTRODUCTION

The time evolution of a quantum system in contact with its environment is commonly described using a master equation (ME) for the system's reduced density operator ρ. A ME having a unique steady state solution is said to be monostable. The widely employed Gorini-Kossakowski-Sudarshan-Lindblad (GKSL) ME [1–3], which is linear in ρ, is monostable, provided that the Hamiltonian is time independent. For such Hamiltonians, the Grabert ME, which has a nonlinear dependency on ρ, is also monostable (its unique steady state solution is thermal equilibrium) [4,5].

In contrast, some experimentally observed behaviors in quantum systems suggest multistability in the underlying dynamics. For example, consider a single-domain ferromagnet under the influence of a transverse (with respect to the domain's easy axis) static magnetic field. Above a critical temperature T_c, the system is monostable. However, a phase transition (PT) occurs at T_c, below which the magnetization has two locally stable steady states. Both the PT and the multistability cannot be derived from any monostable ME.

More generally, for any finite system having a static (i.e., time-independent) Hamiltonian, both PTs and multistabilities cannot be derived from any monostable ME [6–11]. The term finite commonly refers to one out of two of the system's properties. The first property is the number of particles, and the second one is Hilbert space dimensionality. Exclusion of PTs holds for both definitions of this term [12]. On the other hand, all experimental observations of PTs are performed using finite systems. Moreover, a PT has been experimentally observed in small systems, including molecular magnets [13–16].

For some cases, the time evolution of a given dynamical system (i.e., a system having a time-dependent Hamiltonian) can be described using a static (i.e., time-independent) Hamiltonian. For example, when the rotating-wave approximation (RWA) is applicable, a transformation into a rotating frame yields a static Hamiltonian. Similarly to the case of static systems, multistability can be theoretically excluded, provided that the system is finite and the RWA is applicable (see Appendix B of Ref. [17]). In contrast, multistability has been experimentally observed in dynamical spin systems (for which both the number of particles and Hilbert space dimensionality are finite) [18]. One example is a dynamical instability (DI) induced by parallel pumping applied to a ferrimagnetic insulator containing a finite (though commonly large) number of spins [19–21]. In these experiments, the parallel pumping angular frequency is tuned close to $2\omega_L$, where ω_L is the spins' resonance angular frequency. For a driving amplitude ω_1 smaller than a critical value $\omega_{1,c}$ (instability threshold), the system's response is monostable. However, at $\omega_{1,c}$ a bifurcation occurs, above which the spins oscillate with a relative phase ϕ, which is either $\phi = 0$ or $\phi = \pi$.

Theoretical models, which have been developed to account for experimentally observed multistability in finite quantum systems, are usually based on the assumption that the underlying dynamics is nonlinear. Commonly, such nonlinearity is introduced by implementing the mean-field approximation (MFA). It has been shown that the MFA yields both PTs [12] and DIs [22–27] in finite systems. The MFA is based on the assumption that entanglement between subsystems can be disregarded. However, it has remained unclear how such an assumption can be justified within the framework of standard quantum mechanics (QM) [28–30], particularly for cases where the MFA turns a given monostable time evolution into a multistable one.

A modified ME has been recently proposed [31]. This ME [see Eq. (1) below] has an added nonlinear term [32,33] given by $-\Theta\rho - \rho\Theta + 2\langle\Theta\rangle\rho$, which can give rise to both disentanglement and thermalization. Under some appropriate conditions, the ME (1) becomes multistable. The dynamics generated by the modified ME (1) is explored below for a system made of a finite number of coupled spins. It is found that the interplay between an externally applied static magnetic field and the dipolar coupling between spins gives rise to a

*Contact author: eyal@ee.technion.ac.il

PT, which separates a region of monostability and a region of bistability. Moreover, when an externally applied parametric excitation (parallel pumping) is added, the modified ME (1) yields a DI, above which a periodic limit cycle occurs.

II. NONLINEAR ME

The proposed modified ME is given by [31,34,35]

$$\frac{d\rho}{dt} = i\hbar^{-1}[\rho, \mathcal{H}] - \Theta\rho - \rho\Theta + 2\langle\Theta\rangle\rho, \tag{1}$$

where $\hbar$ is the Planck's constant, $\mathcal{H} = \mathcal{H}^\dagger$ is the Hamiltonian, the operator $\Theta = \Theta^\dagger$ is allowed to depend on ρ, and $\langle\Theta\rangle = \mathrm{Tr}(\Theta\rho)$. For the case $\mathcal{H} = 0$, and for a fixed Θ, the modified master equation (1) yields an equation of motion for $\langle\Theta\rangle$ given by $\mathrm{d}\langle\Theta\rangle/\mathrm{d}t = -2\langle(\Theta - \langle\Theta\rangle)^2\rangle$, which implies that the expectation value $\langle\Theta\rangle$ monotonically decreases with time. Hence, the nonlinear term in the modified ME (1) can be employed to suppress a given physical property, provided that $\langle\Theta\rangle$ quantifies that property. The operator Θ is assumed to be given by $\Theta = \gamma_\mathrm{H}\mathcal{Q}^{(\mathrm{H})} + \gamma_\mathrm{D}\mathcal{Q}^{(\mathrm{D})}$, where both rates γ_H and γ_D are positive, and both operators $\mathcal{Q}^{(\mathrm{H})}$ and $\mathcal{Q}^{(\mathrm{D})}$ are Hermitian. The first term $\gamma_\mathrm{H}\mathcal{Q}^{(\mathrm{H})}$ gives rise to thermalization [4,5], whereas the second one $\gamma_\mathrm{D}\mathcal{Q}^{(\mathrm{D})}$ gives rise to disentanglement.

The thermalization operator is given by $\mathcal{Q}^{(\mathrm{H})} = \beta\mathcal{U}_\mathrm{H}$, where $\mathcal{U}_\mathrm{H} = \mathcal{H} + \beta^{-1}\ln\rho$ is the Helmholtz free-energy operator, $\beta = 1/(k_\mathrm{B}T)$ is the thermal energy inverse, k_B is the Boltzmann's constant, and T is the temperature. The thermal equilibrium density operator $\rho_0 = e^{-\beta\mathcal{H}}/\mathrm{Tr}(e^{-\beta\mathcal{H}})$, which minimizes the Helmholtz free energy $\langle\mathcal{U}_\mathrm{H}\rangle$, is a steady state solution of the ME (1), provided that $\gamma_\mathrm{D} = 0$ (i.e., no disentanglement) and the Hamiltonian $\mathcal{H}$ is time independent [4,5,36,37]. The construction of the disentanglement operator $\mathcal{Q}^{(\mathrm{D})}$ is explained in Ref. [31].

III. SPIN PT

The one-dimensional transverse Ising model (TIM) Hamiltonian is given by [38–42]

$$\mathcal{H} = -B\sum_{l=1}^{L}\sigma_{l,z} - J\sum_{l=1}^{L}\sigma_{l,x}\sigma_{l+1,x}, \tag{2}$$

where both B and J are real non-negative constants. The number of spins, which is assumed to be finite, is denoted by L, and the Pauli vector operator $(\sigma_{l,x}, \sigma_{l,y}, \sigma_{l,z})$ represents the lth spin angular momentum in units of $\hbar/2$, where $l \in \{1, 2, \ldots, L\}$. It is assumed that the one-dimensional spin array has a ring configuration, and thus the last ($l = L$) coupling term $\sigma_{l,x}\sigma_{l+1,x}$ [see Eq. (2)] is taken to be given by $\sigma_{L,x}\sigma_{1,x}$.

For the two-spin case (i.e., $L = 2$), the matrix representation of $\mathcal{H}$ in the basis $\{|-1,-1\rangle, |-1,1\rangle, |1,-1\rangle, |1,1\rangle\}$ is given by

$$\mathcal{H} \doteq -2\begin{pmatrix} B & 0 & 0 & J \\ 0 & 0 & J & 0 \\ 0 & J & 0 & 0 \\ J & 0 & 0 & -B \end{pmatrix}, \tag{3}$$

where the ket vector $|\sigma_2, \sigma_1\rangle$ is an eigenvector of $\sigma_{l,z}$ with an eigenvalue $\sigma_l \in \{-1, 1\}$, and where $l \in \{1, 2\}$. Steady state solutions of the modified ME (1) are shown for this case in Fig. 1 as a function of the ratio J/B. The magnetization $\langle\sigma_x\rangle = \langle\sigma_{1,x}\rangle + \langle\sigma_{2,x}\rangle$, which is plotted in Fig. 1(a), becomes finite above a critical value of the ratio J/B (which depends on the rates γ_H and γ_D and on the temperature). The plot in Fig. 1(b) depicts the two-spin entanglement [43–47] $\tau = \langle\mathcal{Q}^{(\mathrm{D})}\rangle$ [see Eq. (11) of Ref. [31]]. Note that τ peaks near the PT.

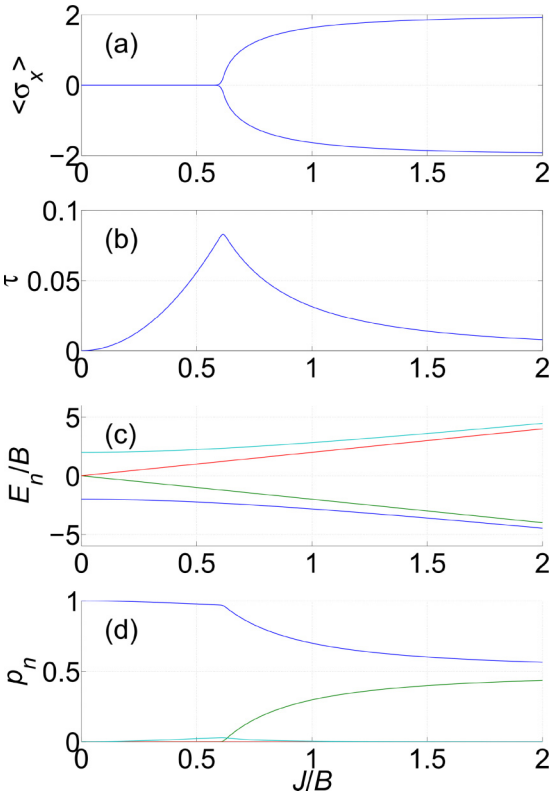

FIG. 1. Two-spin PT. (a) The magnetization $\langle\sigma_x\rangle$, (b) two-spin entanglement τ, (c) energy eigenvalues E_n, and (d) population probabilities p_n, are plotted as a function of the ratio J/B. Assumed parameters' values are $\hbar\gamma_\mathrm{H}/B = 50$ and $\hbar\gamma_\mathrm{D}\beta^{-1}/B^2 = 100$.

Standard QM predicts that $\langle\sigma_x\rangle = 0$ in steady state [note that the Hamiltonian $\mathcal{H}$ (2) is invariant under the mirror reflection $x \to -x$, and consequently, $\langle n|\sigma_x|n\rangle = 0$ for all energy eigenvectors $|n\rangle$]. In contrast, nonvanishing values for $\langle\sigma_x\rangle$ in steady state become possible in the presence of spontaneous disentanglement [see Fig. 1(a)]. For the TIM, the assumption that the MFA is applicable leads to magnetization $\langle\sigma_x\rangle_\mathrm{MFA}$ given by [40]

$$\langle\sigma_x\rangle_\mathrm{MFA} = \begin{cases} 0, & \text{for } \frac{2J}{B} < 1, \\ \pm\sqrt{1 - \left(\frac{B}{2J}\right)^2}, & \text{for } \frac{2J}{B} \geqslant 1. \end{cases} \tag{4}$$

However, as has been discussed above, it has remained unclear how the MFA can be justified within the framework of standard QM. Even though both MFA and spontaneous disentanglement can account for multistability, their predictions are distinguishable, as is discussed below.

The relation $\Theta = \gamma_\mathrm{H}\mathcal{Q}^{(\mathrm{H})} + \gamma_\mathrm{D}\mathcal{Q}^{(\mathrm{D})}$ together with the ME (1) suggest that disentanglement can be accounted for by replacing the Helmholtz free energy $\langle\mathcal{U}_\mathrm{H}\rangle$ by an effective free energy $\langle\mathcal{U}_\mathrm{eff}\rangle$, which is given by $\langle\mathcal{U}_\mathrm{eff}\rangle = \langle\mathcal{U}_\mathrm{H}\rangle +$

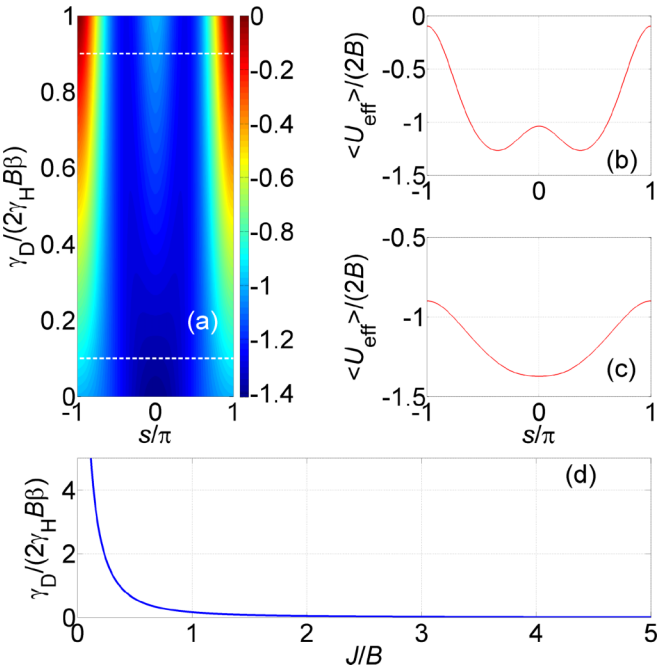

FIG. 2. The effective free energy $\langle \mathcal{U}_{\rm eff}\rangle$. (a) Dependency of $\langle \mathcal{U}_{\rm eff}\rangle$ on $\gamma_{\rm D}/(2\gamma_{\rm H}B\beta)$ and s. The cross-section plots (c) and (b) demonstrate the regions of monostability and bistability, respectively. The overlaid white dotted lines in (a) indicate the two values of the ratio $\gamma_{\rm D}/(2\gamma_{\rm H}B\beta)$ corresponding to the cross-section plots in (b) and (c). For (a)–(c) it is assumed that $J/B = 1$. (d) The critical value of the ratio $\gamma_{\rm D}/(2\gamma_{\rm H}B\beta)$ as a function of J/B.

$\beta^{-1}(\gamma_{\rm D}/\gamma_{\rm H})\langle \mathcal{Q}^{(\rm D)}\rangle$. Consider the case where the temperature is sufficiently low to validate the approximation $\langle \mathcal{U}_{\rm H}\rangle \simeq \langle \mathcal{H}\rangle$. The energy eigenvectors of the two-spin Hamiltonian (3) are denoted by $|1\rangle$, $|2\rangle$, $|3\rangle$, and $|4\rangle$, and the corresponding eigenenergies by $E_1 = -2\sqrt{B^2+J^2}$, $E_2 = -2J$, $E_3 = 2J$, and $E_4 = 2\sqrt{B^2+J^2}$ [see, respectively, blue, green, red, and cyan lines in Fig. 1(c)]. As can be seen from the red and cyan lines in Fig. 1(d), the probabilities p_3 and p_4 to occupy the energy eigenstates $|3\rangle$ and $|4\rangle$ are relatively small both below and above the PT. Consider a class of pure states, for which only the two lowest-energy states are occupied. A state $|\psi\rangle$ belonging to this class is expressed as $|\psi\rangle = e^{i\varphi/2}\sqrt{(1+\cos s)/2}|1\rangle + e^{-i\varphi/2}\sqrt{(1-\cos s)/2}|2\rangle$, where both φ and s are real. With the help of Eq. (15) of Ref. [31], the effective free energy $\langle \mathcal{U}_{\rm eff}\rangle$ can be analytically calculated for this class of pure states. Note that for a given s, the entanglement $\langle\psi|\mathcal{Q}^{(\rm D)}|\psi\rangle$ is minimized for $\varphi = 0$, and that the energy expectation value $\langle\psi|\mathcal{H}|\psi\rangle$ does not depend on the phase φ. Thus, for the current case, the minimization of the effective free energy $\langle \mathcal{U}_{\rm eff}\rangle$ can be simplified by setting $\varphi = 0$. Note that the magnetization $\langle\sigma_x\rangle$ for this setting is given by $\langle\sigma_x\rangle = 2(1+e^{-2\sinh^{-1}(J/B)})^{-1/2}\sin s$. The color-coded plot in Fig. 2(a) depicts the dependency of the effective free energy $\langle \mathcal{U}_{\rm eff}\rangle$ on the ratio $\gamma_{\rm D}/(2\gamma_{\rm H}B\beta)$ and on the parameter s (for $\varphi = 0$). The plot reveals a PT from monostability to bistability occurring at a critical value of the ratio $\gamma_{\rm D}/(2\gamma_{\rm H}B\beta)$. The region of monostability is demonstrated by the plot in Fig. 2(c), whereas bistability is demonstrated by the plot in Fig. 2(b). The two values of the ratio $\gamma_{\rm D}/(2\gamma_{\rm H}B\beta)$ corresponding to the plots in Figs. 2(b) and 2(c) are indicated by the overlaid white dotted lines in Fig. 2(a).

Stability analysis is employed to extract the critical value of the ratio $\gamma_{\rm D}/(2\gamma_{\rm H}B\beta)$ from the effective free energy $\langle \mathcal{U}_{\rm eff}\rangle$. The plot shown in Fig. 2(d) depicts the ratio $\gamma_{\rm D}/(2\gamma_{\rm H}B\beta)$ as a function of J/B at the PT. While the MFA yields a constant value for J/B at the PT [see Eq. (4)], disentanglement makes this value becoming dependent on the rate $\gamma_{\rm D}$ [see Fig. 2(d)]. Moreover, in the region where $\langle\sigma_x\rangle \neq 0$, the magnetization $\langle\sigma_x\rangle$ dependency on the ratio J/B according to the spontaneous disentanglement hypothesis [see Fig. 1(a)] is distinguishable from the one that is derived from the MFA [see Eq. (4)].

Only nearest-neighbor spins are coupled in the TIM [see Eq. (2)]. The disentanglement operator $\mathcal{Q}^{(\rm D)}$ for the case $L > 2$ (i.e., for more than two spins) is accordingly constructed, by including only nearest-neighbor terms. The case $L = 5$ is demonstrated by the plots shown in Figs. 3 and 4. The time evolution of the single-spin Bloch vector $\mathbf{k}_l = (\langle\sigma_{l,x}\rangle, \langle\sigma_{l,y}\rangle, \langle\sigma_{l,z}\rangle)$ is shown in Fig. 3(1), where $l \in \{1, 2, 3, 4, 5\}$. These plots demonstrate flow towards a locally stable steady state with positive magnetization $\langle\sigma_x\rangle$. A state with the opposite magnetization value is also locally stable. The entire Hilbert space is divided into two basins of attraction associated with these two locally stable steady states.

For the case $L = 5$, each spin has two nearest neighbors, and two second nearest neighbors (see the inset of Fig. 4). The time evolution of the entanglement variable τ for all spin pairs is shown in the plot in Fig. 4. Plots corresponding to nearest- (second-nearest-) neighbor pairs are blue (cyan) colored. The shared steady state value of τ for all nearest-neighbor pairs, which is denoted by $\tau_{\rm NN}$, is found to be larger than the shared steady state value of τ for all second-nearest-neighbor pairs, which is denoted by $\tau_{\rm SNN}$ ($\tau_{\rm NN}/\tau_{\rm SNN} \simeq 1.11$ for the example shown in Fig. 4).

IV. SPIN PARAMETRIC INSTABILITY

Disentanglement-induced multistability is explored below for a system made of two spins under parallel pumping. The time-dependent Hamiltonian $\mathcal{H}$ is given by

$$\frac{\mathcal{H}}{\hbar} = \frac{\omega_z\sigma_z}{2} + \omega_{\rm L}\vartheta\frac{\sigma_y^2 - \sigma_x^2}{4}, \tag{5}$$

where $\omega_z = -\omega_{\rm L} + \omega_1\cos(2\omega_{\rm L}t)$. The Larmor angular frequency $\omega_{\rm L}$, the longitudinal driving amplitude ω_1, and the (assumed small) demagnetization asymmetry factor ϑ [48] are all real constants, and $\sigma_i = \sigma_{1,i} + \sigma_{2,i}$ for $i \in \{x, y, z\}$. Note that the term in Eq. (5) proportional to $\sigma_y^2 - \sigma_x^2$ generates squeezing [49–51]. In the RWA, the time-dependent laboratory frame Hamiltonian $\mathcal{H}$ is transformed into a time-independent rotating frame Hamiltonian $\mathcal{H}_{\rm RWA}$, which has a matrix representation given by [see Eq. (17.212) of Ref. [52], and compare to Eq. (3)]

$$\frac{\mathcal{H}_{\rm RWA}}{\hbar} \doteq -2\begin{pmatrix} \mathcal{B} & 0 & 0 & \mathcal{J} \\ 0 & 0 & 0 & 0 \\ 0 & 0 & 0 & 0 \\ \mathcal{J} & 0 & 0 & -\mathcal{B} \end{pmatrix} + O(\vartheta^2), \tag{6}$$

where $\mathcal{B} = -\omega_1/2$ and $\mathcal{J} = -\omega_1\vartheta/4$.

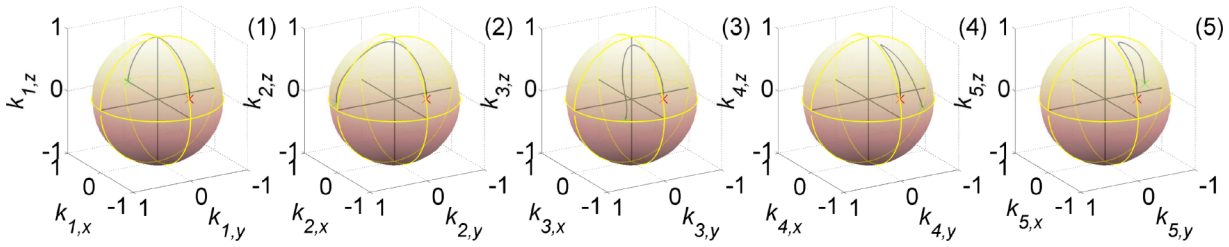

FIG. 3. Five-spin TIM. The green (red) cross symbols represent initial (final) values of the single-spin Bloch vectors. Initially the spins are in a product state, where the lth spin is pointing in the direction $[\cos[2\pi(l-1)/L], \sin[2\pi(l-1)/L], 0]$. Parameters' assumed values are $J/B = 2$, $\hbar\gamma_{\mathrm{H}}/B = 5$, and $\hbar\gamma_{\mathrm{D}}\beta^{-1}/B^2 = 100$.

As can be seen from Eq. (6), $\mathcal{H}_{\mathrm{RWA}}$ becomes diagonal when the demagnetization asymmetry factor ϑ vanishes. This behavior is attributed to the observation that for $\vartheta = 0$ there is no preferred direction in the plane perpendicular to the constant magnetic field (the xy plane). Thus, for $\vartheta = 0$ the relative phase ϕ of precession with respect to the parametric driving has no preferred value. On the other hand, for finite ϑ, the relative phase ϕ has two preferred values denoted by $\phi_1 = 0$ and $\phi_2 = \pi$.

The time evolution of the Bloch vector $\mathbf{k} = (\langle\sigma_x\rangle, \langle\sigma_y\rangle, \langle\sigma_z\rangle)$ is shown in Figs. 5(c) and 5(d). As is demonstrated by the plot in Fig. 5(c), in the absence of disentanglement (i.e., $\gamma_{\mathrm{D}} = 0$), the steady state is a fixed point. By turning on disentanglement (all other parameters are kept unchanged), the steady state becomes a periodic limit cycle, as is demonstrated by the plot in Fig. 5(d). The dependency on the ratio $\mathcal{J}/\mathcal{B}$ of the magnetization $\langle\sigma_x\rangle$ and the two-spin entanglement τ is shown in Figs. 5(a) and 5(b), respectively. Due to the similarity between the Hamiltonians (3) and (6), the underlying mechanism responsible for the instability seen in Fig. 5, is similar to the one seen in Fig. 1.

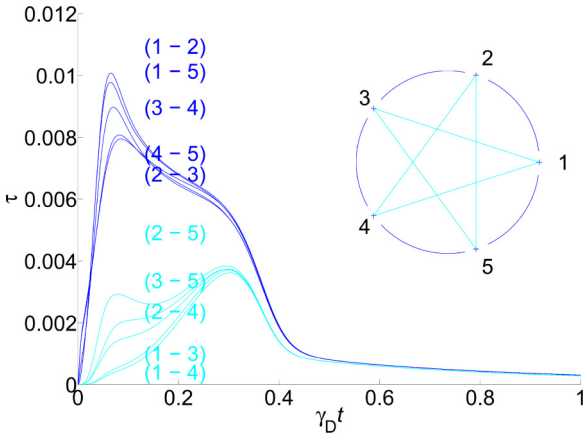

FIG. 4. Pair entanglement τ. Plots corresponding to nearest- (second-nearest-) neighbor pairs are blue (cyan) colored. Parameters' assumed values are listed in the caption of Fig. 3. The number of both nearest- and second-nearest-neighbor pairs is $L = 5$. The initial product state at $\gamma_{\mathrm{D}}t = 0$, for which entanglement of all pairs vanishes, is associated with the five green cross symbols shown in Fig. 3. As is shown in Fig. 3, initially all five single-spin Bloch vectors move from their initial values along the equator towards the north pole of their Bloch spheres. This process corresponds to the time interval of $0 < \gamma_{\mathrm{D}}t \lesssim 0.3$. The limit $\gamma_{\mathrm{D}}t \to \infty$ is represented by the five red crosses in Fig. 3.

V. DISCUSSION

The current study explores multistability generated by the modified master equation given by Eq. (1). The proposed modified master equation (1) can be constructed for any physical system whose Hilbert space has finite dimensionality. Any candidate master equation modification has to satisfy some legitimizing properties. For the master equation given by Eq. (1), the condition $\mathrm{d}\,\mathrm{Tr}\,\rho/\mathrm{d}t = 0$ holds provided that $\mathrm{Tr}\,\rho = 1$ (i.e., ρ is normalized), and $\mathrm{d}\,\mathrm{Tr}\,\rho^2/\mathrm{d}t = 0$, provided that $\rho^2 = \rho$ (i.e., ρ represents a pure state). The first property guaranties norm conservation, whereas positive-semidefiniteness of ρ is ensured by the second property, together with the relation $\mathrm{d}\ln(\det\rho)/\mathrm{d}t = -2\,\mathrm{Tr}(\Theta - \langle\Theta\rangle)$ [see Eq. (2.196) of Ref. [52]].

Suppression of entanglement (i.e., disentanglement) is introduced using the operator $\mathcal{Q}^{(\mathrm{D})}$ [31]. The added disentanglement term makes the collapse postulate of QM redundant. This nonlinear term has no effect on any product (i.e., disentangled) state. For a multipartite system, disentanglement

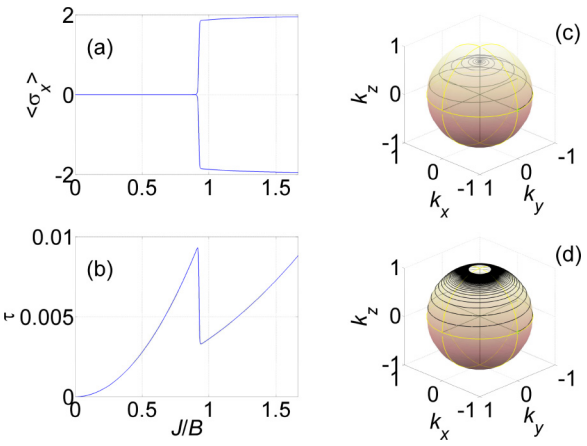

FIG. 5. Parallel pumping. (a) The magnetization $\langle\sigma_x\rangle$ and (b) two-spin entanglement τ in steady state are plotted as a function of the ratio $\mathcal{J}/\mathcal{B}$. Assumed parameters' values are $\hbar\gamma_{\mathrm{H}}/\mathcal{B} = 5$ and $\hbar\gamma_{\mathrm{D}}\beta^{-1}/\mathcal{B}^2 = 100$. The green cross symbols in (c) and (d) represent initial values of the Bloch vector. While disentanglement is inactive (i.e., $\gamma_{\mathrm{D}} = 0$) in (c), the dimensionless disentanglement rate is $\hbar\gamma_{\mathrm{D}}\beta^{-1}/\mathcal{B}^2 = 100$ in (d). For both (c) and (d), $\mathcal{J}/\mathcal{B} = 1.05$.

between any pair of subsystems can be introduced. The expectation value $\langle \mathcal{Q}^{(\mathrm{D})} \rangle$ is invariant under any subsystem unitary transformation. The disentanglement operator $\mathcal{Q}^{(\mathrm{D})}$ can be constructed for both distinguishable [31] and indistinguishable particles [53]. Moreover, thermalization can be incorporated using the operator $\mathcal{Q}^{(\mathrm{H})}$.

VI. SUMMARY

The current study is motivated by an apparent discrepancy between some experimental observations and the standard theory of QM. Multistability has been experimentally observed in a variety of quantum systems. On the other hand, in standard QM the time evolution is governed by a monostable ME. For some cases, it has remained unclear how multistability can be theoretically derived from standard QM.

The spontaneous disentanglement hypothesis is inherently falsifiable, because it yields predictions, which are experimentally distinguishable from predictions obtained from standard QM. It is found that multistability can be obtained in the presence of spontaneous disentanglement. In particular, the modified ME (1) yields a PT for the TIM (see Figs. 1–3), and a DI for the longitudinally driven spins (see Fig. 5). These theoretical findings, together with experimental observations of multistability in finite quantum systems, indirectly support the hypothesis that spontaneous disentanglement occurs in quantum systems.

ACKNOWLEDGMENTS

Useful discussions with Michael Reznikov are acknowledged.

[1] B. Fernengel and B. Drossel, Bifurcations and chaos in nonlinear Lindblad equations, J. Phys. A: Math. Theor. **53**, 385701 (2020).
[2] G. Lindblad, On the generators of quantum dynamical semigroups, Commun. Math. Phys. **48**, 119 (1976).
[3] D. Manzano, A short introduction to the Lindblad master equation, AIP Adv. **10**, 025106 (2020).
[4] H. Grabert, Nonlinear relaxation and fluctuations of damped quantum systems, Z. Phys. B **49**, 161 (1982).
[5] H. C. Öttinger, Nonlinear thermodynamic quantum master equation: Properties and examples, Phys. Rev. A **82**, 052119 (2010).
[6] P. Chomaz and F. Gulminelli, Phase transitions in finite systems, in *Dynamics and Thermodynamics of Systems with Long-Range Interactions* (Springer, Berlin, 2002), pp. 68–129.
[7] P. Mainwood, Phase transitions in finite systems (2005), https://philsci-archive.pitt.edu/8340/.
[8] C. Callender, Taking thermodynamics too seriously, Stud. Hist. Philos. Sci. B **32**, 539 (2001).
[9] C. Liu, Explaining the emergence of cooperative phenomena, Philos. Sci. **66**, S92 (1999).
[10] V. Ardourel and S. Bangu, Finite-size scaling theory: Quantitative and qualitative approaches to critical phenomena, Stud. Hist. Philos. Sci. **100**, 99 (2023).
[11] E. Shech, What is the paradox of phase transitions? Philos. Sci. **80**, 1170 (2013).
[12] M. Toda, R. Kubo, N. Saitō, N. Hashitsume, and N. Hashitsume, *Statistical Physics I* (Springer, Berlin, 1978).
[13] N. Roch, S. Florens, V. Bouchiat, W. Wernsdorfer, and F. Balestro, Quantum phase transition in a single-molecule quantum dot, Nature (London) **453**, 633 (2008).
[14] L. Thomas, F. L. Lionti, R. Ballou, D. Gatteschi, R. Sessoli, and B. Barbara, Macroscopic quantum tunnelling of magnetization in a single crystal of nanomagnets, Nature (London) **383**, 145 (1996).
[15] S. Trishin, C. Lotze, N. Bogdanoff, F. von Oppen, and K. J. Franke, Moiré tuning of spin excitations: Individual Fe atoms on MoS_2/Au (111), Phys. Rev. Lett. **127**, 236801 (2021).
[16] G. G. Blesio and A. A. Aligia, Topological quantum phase transition in individual Fe atoms on MoS_2/Au (111), Phys. Rev. B **108**, 045113 (2023).
[17] R. Levi, S. Masis, and E. Buks, Instability in the Hartmann-Hahn double resonance, Phys. Rev. A **102**, 053516 (2020).
[18] A. G. Gurevich and G. A. Melkov, *Magnetization Oscillations and Waves* (CRC Press, Boca Raton, FL, 2020).
[19] H. Suhl, The theory of ferromagnetic resonance at high signal powers, J. Phys. Chem. Solids **1**, 209 (1957).
[20] E. Schlömann, R. I. Joseph, and I. Bady, Spin-wave instability in hexagonal ferrites with a preferential plane, J. Appl. Phys. **34**, 672 (1963).
[21] A. A. Zvyagin, Modulation of the longitudinal pumping in quantum spin systems, Phys. Rev. B **101**, 174408 (2020).
[22] E. Schlömann, J. J. Green, and U. Milano, Recent developments in ferromagnetic resonance at high power levels, J. Appl. Phys. **31**, S386 (1960).
[23] H.-P. Breuer, F. Petruccione *et al.*, *The Theory of Open Quantum Systems* (Oxford University Press, Oxford, U.K., 2002).
[24] B. Drossel, What condensed matter physics and statistical physics teach us about the limits of unitary time evolution, Quantum Stud.: Math. Found. **7**, 217 (2020).
[25] C. Hicke and M. I. Dykman, Classical dynamics of resonantly modulated large-spin systems, Phys. Rev. B **78**, 024401 (2008).
[26] W. Kłobus, P. Kurzyński, M. Kuś, W. Laskowski, R. Przybycień, and K. Życzkowski, Transition from order to chaos in reduced quantum dynamics, Phys. Rev. E **105**, 034201 (2022).
[27] M. R. Hush, W. Li, S. Genway, I. Lesanovsky, and A. D. Armour, Spin correlations as a probe of quantum synchronization in trapped-ion phonon lasers, Phys. Rev. A **91**, 061401 (2015).
[28] V. Vedral, Mean-field approximations and multipartite thermal correlations, New J. Phys. **6**, 22 (2004).
[29] D. A. R. Sakthivadivel, Magnetisation and mean field theory in the Ising model, SciPost Physi. Lect. Notes **1**, 35 (2022).
[30] C. Osácar and A. F. Pacheco, A mean field approach to the Ising chain in a transverse magnetic field, Eur. J. Phys. **38**, 045404 (2017).
[31] E. Buks, Spontaneous disentanglement and thermalization, Adv. Quantum Technol. **7**, 2400036 (2024).
[32] D. E. Kaplan and S. Rajendran, Causal framework for nonlinear quantum mechanics, Phys. Rev. D **105**, 055002 (2022).

[33] M. R. Geller, Fast quantum state discrimination with nonlinear positive trace-preserving channels, Adv. Quantum Technol. **6**, 2200156 (2023).
[34] R. Grimaudo, A. De Castro, M. Kuś, and A. Messina, Exactly solvable time-dependent pseudo-Hermitian su(1,1) Hamiltonian models, Phys. Rev. A **98**, 033835 (2018).
[35] K. Kowalski and J. Rembieliński, Integrable nonlinear evolution of the qubit, Ann. Phys. **411**, 167955 (2019).
[36] E. T. Jaynes, The minimum entropy production principle, Annu. Rev. Phys. Chem. **31**, 579 (1980).
[37] E. Buks and D. Schwartz, Stability of the Grabert master equation, Phys. Rev. A **103**, 052217 (2021).
[38] E. Lieb, T. Schultz, and D. Mattis, Two soluble models of an antiferromagnetic chain, Ann. Phys. **16**, 407 (1961).
[39] P. Pfeuty, The one-dimensional Ising model with a transverse field, Ann. Phys. **57**, 79 (1970).
[40] G. B. Mbeng, A. Russomanno, and G. E. Santoro, The quantum Ising chain for beginners, SciPost Phys. Lect. Notes, 82 (2024).
[41] D. Nagaj, E. Farhi, J. Goldstone, P. Shor, and I. Sylvester, Quantum transverse-field Ising model on an infinite tree from matrix product states, Phys. Rev. B **77**, 214431 (2008).
[42] B. K. Chakrabarti, A. Dutta, and P. Sen, *Quantum Ising Phases and Transitions in Transverse Ising Models*, Vol. 41 (Springer, Berlin, 2008).
[43] G. R. Grimmett, T. J. Osborne, and P. F. Scudo, Entanglement in the quantum Ising model, J. Stat. Phys. **131**, 305 (2008).
[44] C.-M. Jian, B. Bauer, A. Keselman, and A. W. W. Ludwig, Criticality and entanglement in nonunitary quantum circuits and tensor networks of noninteracting fermions, Phys. Rev. B **106**, 134206 (2022).
[45] J. I. Latorre, E. Rico, and G. Vidal, Ground state entanglement in quantum spin chains, Quantum Inf. Comput. **4**, 48 (2004).
[46] T. J. Osborne and M. A. Nielsen, Entanglement in a simple quantum phase transition, Phys. Rev. A **66**, 032110 (2002).
[47] G. Parez and W. Witczak-Krempa, The fate of entanglement, arXiv:2402.06677.
[48] C. Kittel *et al.*, *Introduction to Solid State Physics*, Vol. 8 (Wiley New York, 1976).
[49] J. Kitzinger, M. Chaudhary, M. Kondappan, V. Ivannikov, and T. Byrnes, Two-axis two-spin squeezed states, Phys. Rev. Res. **2**, 033504 (2020).
[50] M. Kitagawa and M. Ueda, Squeezed spin states, Phys. Rev. A **47**, 5138 (1993).
[51] J. Ma, X. Wang, C.-P. Sun, and F. Nori, Quantum spin squeezing, Phys. Rep. **509**, 89 (2011).
[52] E. Buks, Quantum mechanics - Lecture Notes, http://buks.net.technion.ac.il/teaching/ (2024).
[53] E. Buks (unpublished).